First publ. in: Journal of Biological Chemistry 279 (2004), 28, pp. 29718–29727

Structure-Function Correlation in Glycine Oxidase from *Bacillus subtilis**

Received for publication, February 4, 2004, and in revised form, April 20, 2004
Published, JBC Papers in Press, April 22, 2004, DOI 10.1074/jbc.M401224200

Mario Mörtl‡, Kay Diederichs‡, Wolfram Welte‡, Gianluca Molla§, Laura Motteran§, Gabriella Andriolo§, Mirella S. Pilone§, and Loredano Pollegioni§¶

From the ‡Section of Biology, University of Konstanz, P. O. Box 5560-M656 and the §Department of Structural and Functional Biology, University of Insubria, via J. H. Dunant 3, 21100 Varese, Italy

Structure-function relationships of the flavoprotein glycine oxidase (GO), which was recently proposed as the first enzyme in the biosynthesis of thiamine in *Bacillus subtilis*, has been investigated by a combination of structural and functional studies. The structure of the GO-glycolate complex was determined at 1.8 Å, a resolution at which a sketch of the residues involved in FAD binding and in substrate interaction can be depicted. GO can be considered a member of the "amine oxidase" class of flavoproteins, such as D-amino acid oxidase and monomeric sarcosine oxidase. With the obtained model of GO the monomer-monomer interactions can be analyzed in detail, thus explaining the structural basis of the stable tetrameric oligomerization state of GO, which is unique for the GR_2 subfamily of flavooxidases. On the other hand, the three-dimensional structure of GO and the functional experiments do not provide the functional significance of such an oligomerization state; GO does not show an allosteric behavior. The results do not clarify the metabolic role of this enzyme in *B. subtilis*; the broad substrate specificity of GO cannot be correlated with the inferred function in thiamine biosynthesis, and the structure does not show how GO could interact with ThiS, the following enzyme in thiamine biosynthesis. However, they do let a general catabolic role of this enzyme on primary or secondary amines to be excluded because the expression of GO is not inducible by glycine, sarcosine, or D-alanine as carbon or nitrogen sources.

Glycine oxidase (GO,[1] EC 1.4.3.19) is a flavoprotein consisting of four identical subunits (369 residues each) and containing one molecule of noncovalently bound FAD per 42-kDa protein molecule (1, 2). GO catalyzes a reaction similar to that of D-amino acid oxidase (DAAO, EC 1.4.3.3), a paradigm of the dehydrogenase-oxidase class of flavoproteins (for a recent review see Ref. 3). Both enzymes catalyze the oxidative deamination of amino acids to yield the corresponding α-imino acids and, after hydrolysis, α-keto acids, ammonia (or primary amines), and hydrogen peroxide. Both enzymes show a high pK_a for flavin N-3H ionization, do not bind covalently the FAD cofactor, and react readily with sulfite (1–3), but they differ in substrate specificity. In addition to neutral D-amino acids (*e.g.* D-alanine, D-proline, etc., which are also good substrates of DAAO), GO catalyzes the oxidation of primary and secondary amines (*e.g.* glycine, sarcosine, etc.) partially sharing the substrate specificity with monomeric sarcosine oxidase (MSOX, EC 1.5.3.1), an enzyme that catalyzes the oxidative demethylation of sarcosine to yield glycine, formaldehyde, and hydrogen peroxide (4). According to investigations of the substrate specificity and of the binding properties, the GO active site seems to preferentially accommodate amines of a small size, such as glycine and sarcosine (1, 2). GO follows a ternary complex sequential mechanism with glycine, sarcosine, and D-proline as substrates in which the rate of product dissociation from the re-oxidized enzyme form represents the rate-limiting step (5). Such a kinetic mechanism is similar to that determined for mammalian DAAO on neutral D-amino acids and for the MSOX on L-proline (6, 7); the main difference is represented by the observed reversibility of the GO reductive half-reaction.

Taken together, however, these results do not really clarify the function of GO in *Bacillus subtilis*; they only outline a general catabolic role for GO (1, 2). Recent work proposed GO as the first enzyme in the biosynthesis of the thiazole moiety of thiamine pyrophosphate cofactor in *B. subtilis* (8). According to this hypothesis, GO catalyzes the oxidation of glycine to give the imine product that would be trapped with the thiocarboxylate intermediate bound to the following enzyme of the pathway (ThiS). In such a mechanism, the nucleophilic addition might occur at the active site of GO to avoid hydrolysis of the imino product. The known 2.3-Å resolution structure of GO (8) does not provide direct evidence of such a reactivity. However, this anabolic function of GO is particularly intriguing because amino acid oxidases are usually involved in the catabolic utilization of their substrates. From this point of view, GO resembles L-aspartate oxidase that converts L-aspartate to iminoaspartate using molecular oxygen or fumarate as electron acceptors, the first reaction in the NAD^+ biosynthesis pathway in bacteria (9). Furthermore, GO is also the object of particular attention because it can be used in an *in vitro* assay, in parallel to DAAO, to detect and modulate the level of glycine or D-serine in the proximity of *N*-methyl-D-aspartic acid receptors in human brain.

Here we report the crystal structure of *B. subtilis* GO in complex with the inhibitor glycolate at 1.8 Å resolution. Al-

* This work was supported by Italian MURST Grant Prot 2002057751 (to M. S. P.), by Fondo di Eccellenza 2001, University of Insubria (to M. S. P.), by FAR 2001 (to L. P.), and by FAR 2002 and 2003 (to M. S. P.). The costs of publication of this article were defrayed in part by the payment of page charges. This article must therefore be hereby marked "*advertisement*" in accordance with 18 U.S.C. Section 1734 solely to indicate this fact.

The atomic coordinates and structure factors (code 1RYI) have been deposited in the Protein Data Bank, Research Collaboratory for Structural Bioinformatics, Rutgers University, New Brunswick, NJ (http://www.rcsb.org/).

¶ To whom correspondence should be addressed. Tel.: 390-332-421506; Fax: 390-332-421500; E-mail: loredano.pollegioni@uninsubria.it.

[1] The abbreviations used are: GO, glycine oxidase; DAAO, D-amino acid oxidase; RgDAAO, *Rhodotorula gracilis* D-amino acid oxidase; pkDAAO, pig kidney D-amino acid oxidase; MSOX, monomeric sarcosine oxidase; GR, glutathione reductase; r.m.s., root mean square; ASU, asymmetric unit.

though the inhibitor was found in an unexpected orientation, active site residues that are likely to bind the substrate or to assist in its oxidation have been tentatively identified on the basis of similarities with other related flavoprotein amine oxidoreductases. In fact, the structures of DAAO, MSOX, and L-amino acid oxidase have also been resolved (10–13); it can thus be expected that comparison of their active sites as well as the mode of interaction with the substrate/ligand would provide insights into the similarities and differences in the structure-function relationships of flavoenzymes active on similar compounds. In addition, and with the aim of clarifying the role of GO in *B. subtilis*, the effect of different carbon and nitrogen sources on cell growth and on the level of GO expression has been investigated.

EXPERIMENTAL PROCEDURES

Growth Conditions and Preparation of Cell Extracts—B. subtilis pre-culture was grown aerobically at 37 °C in the dark and under shaking (180 rpm) on a chemically defined, pH-controlled liquid medium (minimal medium) containing 1× minimal salt solution, 0.4% glucose, 0.005% L-tryptophan, 0.2% L-glutamine, 4 mg/ml $FeCl_3$, 0.2 mg/ml $MnSO_4$, and 1% (v/v) trace element salt solution. The 1× minimal salt solution contained 11.5 mM K_2SO_4, 0.8 mM $MgSO_4$, 6.2 mM K_2HPO_4, and 3.4 mM sodium citrate, pH 7.0. The 1× trace element salt solution contained 43 μM $CaCl_2$, 12.5 μM $ZnCl_2$, 2.5 μM $CuCl_2$, 2.5 μM $CoCl_2$, and 2.5 μM $NaMoO_4$. This pre-culture was then diluted to a final A_{600} ~ 0.08 in 500 ml of minimal medium (2-liter flasks) and grown for 16 h as reported above. The cells were collected by centrifugation, suspended in 2 ml of 1× minimal salt solution, and finally used to inoculate 600 ml of minimal medium supplemented with the appropriate nutrients (initial A_{600} ~ 0.08). Alternatively, a classic M9 medium (containing 1× minimal salt solution, 22 mM glucose, 2 mM $MgSO_4$, and 0.1 mM $CaCl_2$) supplemented with the appropriate nutrient was also used. The cells were grown in flasks as reported above and collected at different growth phases by centrifugation (4000 rpm for 10 min at room temperature) from 100 ml of fermentation broth. Cell growth was followed by absorbance measurements at 600 nm. The crude extracts were prepared according to Ref. 14. In detail, 1 g of cell paste was added to 5 ml of a 2 mg/ml lysozyme solution in TE buffer, pH 8.0, and incubated for 30 min at 37 °C; this sample was then centrifuged at 5000 rpm for 20–30 min at room temperature and 10 ml of lysis buffer added to the pellet (50 mM Tris-HCl, pH 8.0, 1 mM EDTA, 100 mM NaCl, 1.1 mM phenylmethylsulfonyl fluoride, 5 μg/ml DNase I). After 15–30 min of incubation, the crude extract was recovered by centrifugation at 14,500 rpm for 15 min at 4 °C.

Protein Analyses, Enzyme Assay, and Gel-permeation Chromatography—B. subtilis crude extracts were employed for the following assays: (*a*) determination of protein concentration (Biuret method); (*b*) determination of GO activity (polarographic assay, see below); and (*c*) determination of the total GO concentration (by Western blot analysis). A fixed amount of protein (≤300 μg) from the crude extract (the soluble fraction obtained after cell disruption and centrifugation) was separated by SDS-PAGE and electroblotted to a nitrocellulose membrane. The same analysis was also performed on whole cell samples by separation of the proteins corresponding to 240 μl of fermentation broth. GO was detected by immunostaining using monospecific rabbit anti-GO antibodies and visualized using anti-rabbit IgG alkaline phosphatase conjugated with 5-bromo-4-chloro-3-indolyl phosphate and nitro blue tetrazolium chloride, as reported previously (2), or anti-rabbit IgG horseradish peroxidase conjugated with a chemiluminescent substrate (SuperSignal West Pico, Pierce). The amount of anti-GO immunoreactive protein was determined by densitometric analysis using a 50–1000-ng titration curve obtained using pure GO.

Glycine oxidase activity was assayed in a thermostated Hansatech oxygen electrode measuring the oxygen consumption at pH 8.5 and 25 °C with 10 mM sarcosine as substrate (1, 2). One unit of GO is defined as the amount of enzyme that converts 1 μmol of substrate (sarcosine or oxygen) per min at 25 °C.

The oligomerization state of GO was investigated by means of gel-permeation chromatography on a Superdex™ 200 HR 10/30 column (Amersham Biosciences) using 50 mM sodium pyrophosphate, pH 8.5, 5% glycerol, and 250 mM NaCl as elution buffer (1). The pH effect on GO oligomerization state was determined by chromatographic separation using 50 mM potassium phosphate (pH 6.5 and 7.5), 50 mM sodium pyrophosphate (pH 8.5), or 25 mM sodium pyrophosphate and 25 mM sodium carbonate (pH 9.5), all containing 250 mM sodium chloride and 5% (v/v) glycerol.

Limited Proteolysis Experiments—GO (1 mg/ml) was incubated at 25 °C in 50 mM sodium pyrophosphate, pH 8.5, and 1% glycerol with 10% (w/w) trypsin, chymotrypsin, or SV8 protease. For electrophoretic analysis, 1.5 mM phenylmethylsulfonyl fluoride was added to protein samples (10 μg of GO) taken at different times after the addition of protease and immediately frozen for analysis by native PAGE on a 7.5% (w/v) polyacrylamide gel or diluted in the sample buffer for SDS-PAGE, boiled for 3 min, and then loaded on a 12% (w/v) polyacrylamide gel. Gels were stained with Coomassie Blue R-250 and, only for gels from native PAGE, stained for GO activity as reported previously (1). The oligomerization state of proteolyzed GO samples was determined by gel-permeation chromatography (see above), and their N-terminal sequence was determined by means of automated Edman degradation using a Procise protein sequencer (Applied Biosystems).

Preparation of the Protein and Crystallization—Wild-type GO was expressed in *Escherichia coli* using the pT7-HisGO expression system in BL21(DE3)pLysS *E. coli* cells (2). The pT7-HisGO encodes a fully active fusion protein with 13 additional residues at the N terminus of GO (MHHHHHHMARIRA). The purified protein was concentrated up to 15 mg/ml and equilibrated in 50 mM disodium pyrophosphate buffer, pH 8.5, 10% glycerol by gel-permeation chromatography on a Sephadex G-25 (PD10) column.

The recombinant form of GO was crystallized following dynamic light scattering analysis (DynaPro, Protein Solutions Ltd.) by the hanging drop vapor diffusion method, mixing 1 μl of reservoir and 1 μl of protein solution (13 mg/ml) at 18 °C. Crystals with two different space groups were obtained. GO crystals of the space group $P6_122$ were obtained by using a reservoir solution containing 1 M sodium citrate, pH 6.2; the hexagonal crystals grew in 2–3 weeks. Crystals of the space group $C222_1$ were obtained using a GO solution containing 30 mM sodium glycolate and a reservoir solution containing 100 mM imidazole (pH 8.2), 200 mM calcium acetate, and 10% (w/v) PEG 1000; the orthorhombic crystals grew in 1–3 days. Prior to flash-freezing using liquid nitrogen, the crystals were soaked with the corresponding reservoir buffer containing 13% (v/v) ethylene glycol. Heavy atom derivatives were prepared by addition in the reservoir buffer of $KAu(CN)_2$ or $K_2Pt(CN)_4$ to the hexagonal crystal form of GO (1 mM final concentration) and incubating them for 12–16 h. For cryoprotection, the cryoprotectant buffer with an added 1 mM of the corresponding heavy atom salt was used.

Solution of the GO Crystal Structure—All data sets were collected under cryogenic conditions at 100 K. For collecting data of the heavy atom derivatives the MAR345 image plate system with a rotating anode x-ray source (Schneider, Offenburg, Germany) was used. A native data set from the hexagonal crystal was measured at the DESY (EMBL, Hamburg) using the MAR345 image plate system. The 1.8-Å GO-glycolate complex was measured from the orthorhombic crystal at the PSI/SLS (Villigen, Switzerland) using a Mar CCD detector 165 mm in diameter. Space group determination and data reduction were carried out with XDS (15). The programs SOLVE/RESOLVE (16, 17) were used to solve phases by multiple isomorphous replacement. With MOLREP (18), which is part of the CCP4 package (19), and monomeric sarcosine oxidase as a model (Protein Data Bank code 1el5), the position of one of the two molecules per asymmetric unit was found in the map calculated by RESOLVE. The second molecule was positioned using O (20). Alternating refinement in CNS (21) and model building in O was carried out until an R_{free} of 30% was reached. This model was used with MOLREP to find the four molecules in the asymmetric unit of the orthorhombic crystal. The GO-glycolate complex was refined with REFMAC5 (22), and the secondary structure was analyzed with DSSP (definition of secondary structure of proteins given a set of three-dimensional coordinates) (23). For detailed data collection statistics see Table I and for refinement statistics see Table II. Structure plots were produced with the programs MOLSCRIPT (24), RASTER3D (25), and DINO (26).

Comparison of GR Family Members—A superposition of several members of the GR_2 family with GO was performed using the program SUPERIMPOSE (27), and parameters describing the superposition were extracted with LSQMAN (28) from the best topological superposition.

Accession Numbers—The coordinates and structure factors of glycine oxidase in complex with the inhibitor glycolate have been deposited in the Protein Data Bank under accession code 1RYI.

RESULTS

Description of the Structure—The GO protein used for the present investigations is a chimeric protein containing 13 res-

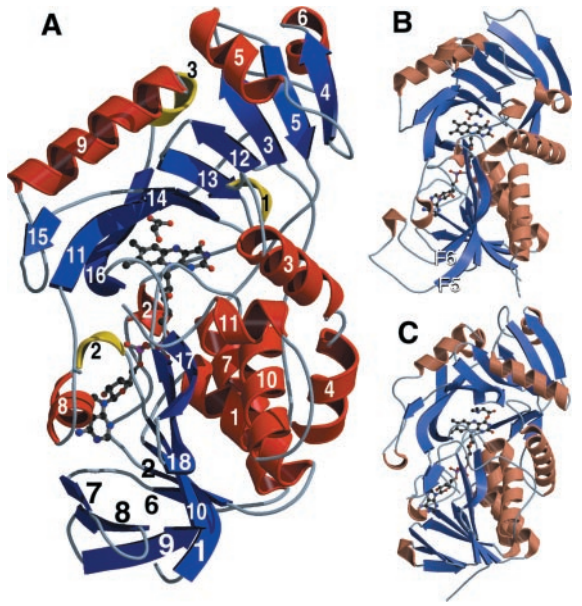

FIG. 1. **Ribbon representation of the GO-glycolate complex (1ryi_a) (*A*), of RgDAAO in complex with D-alanine (*B*), and of MSOX in complex with dimethylglycine (*C*).** Secondary structure elements are highlighted as follows: β-sheets (*blue*), α-helices (*red*), and 3/10 helices (*yellow*).

idues at the N terminus in addition to the 369 amino acids in the native form (1, 2). The structure of the complex obtained in the presence of glycolate at 1.8 Å is depicted in Fig. 1 (see also Tables I and II). A slightly different protein architecture topology of GO has been shown previously (8) using the 2.3-Å resolution structure; the secondary structure topology consists of 14 helices (three small 3/10 helices and 11 regular α-helices) and 18 β-strands (Fig. 2). The position of the residues that initiate and terminate the secondary structure elements is frequently different in our structure compared with the previously shown topology (8). The main difference is represented by the three newly identified 3/10 helices (depicted in *yellow* in Fig. 2); the overall topology is not changed. GO is a two-domain protein, which consists of a FAD-binding domain and a substrate-binding domain. The main structural elements are central antiparallel β-sheets, as first observed in the flavoprotein *p*-hydroxybenzoate hydroxylase (29). The classic FAD-binding domain is common to the glutathione reductase (GR) class of flavoproteins (30). In GO, this motif consists of a six-stranded β-sheet composed of five parallel β-strands (strands 6, 2, 1, 10, and 18) and one additional antiparallel strand (strand 17) and flanked on one side by three α-helices (helices 1, 7, and 10) and on the other side by a three-stranded antiparallel β-sheet (strands 7–9) and a small α-helix (helix 8). The polypeptide chain crosses between the two domains four times (after helix 4, strand 5, helix 8, and strand 16). The most significant differences between the GO structure and both MSOX and RgDAAO are represented by α-helix 8, which is missing in the other two enzymes, a different α-helix 3 and 4 topology, which is fused to a single continuous helix in RgDAAO and MSOX, and by the three stranded β-sheet (strands 7–9 in GO) of the flavin-binding domain, which is conserved in all GR family members and is not conserved in RgDAAO (10, 11) (see Fig. 1). Another main topological difference with RgDAAO is the absence of the loop consisting of 21 amino acids connecting βF5 and βF6 in RgDAAO (Fig. 1*B*), which is involved in monomer-monomer interaction and is not present in other known DAAO sequences (11). Concerning the substrate-binding domain, an element corresponding to α-helix 6 of GO is not conserved in RgDAAO. Analogously to the yeast DAAO, GO shares an active site loop (connecting strands β13 and β14) that is shorter by 5–8 residues as compared with pkDAAO and MSOX.

At the N terminus none of the 13 additional amino acids (MHHHHHHMARIRA) present in recombinant GO can be modeled into the electron density, thus apparently possessing a flexible conformation. At the C terminus, five residues (Glu^{365}, Ala^{366}, Val^{367}, Gln^{368}, and Ile^{369}) protrude out of the protein and are not visible in our model and thus do not appear to interact with any of the other subunits. Most interesting, all GO regions that are involved in monomer-monomer interaction (see below) have low temperature factors. In the loop connecting β7 and β8 of the β-meander (Fig. 1), the electron density for four amino acids (Arg^{180}–Ala^{183}) is weak, indicating that part of the loop is very flexible. The region Ala^{55}–Asp^{60} after helix 2 also shows weak electron density. In MSOX this region corresponds to a flexible loop (Tyr^{55}–Tyr^{61}) that changes from a disordered to a weak electron density following the binding of an active site ligand, thus shielding the positive surface potential at the FAD site (12). This loop, and in particular the side chain of Arg^{52}, was thus suggested to act in MSOX as a switch for active site accessibility (see below).

Homology of GO with Other Amine Oxidoreductases—GO exhibits the highest sequence conservation with the β-subunit of heterotetrameric sarcosine oxidase, sarcosine dehydrogenase, and dimethylglycine dehydrogenase (24–27% identity), less similarity with the sequences of MSOX and pipecolate oxidase (~21% identity), and a modest similarity with DAAO and D-aspartate oxidase (18.4% identity) (2). Furthermore, the primary sequence of GO shows a high degree of conservation with the product of *thiO* gene of *Rhizobium etli* (23.0% of sequence identity). *thiO* is the second open reading frame of four genes (*thiC, thiO, thiG,* and *thiE*) located on plasmid pb, which are involved in the synthesis of thiamine in *R. etli* (31). *R. etli* ThiO protein (a 327-amino acid protein) contains at its N terminus a flavin adenine dinucleotide-binding motif and shares many of the residues involved in the catalytic site of DAAO; it has been also suggested that ThiO may have amino acid oxidase activity (31). In *E. coli* five genes (*thiC, thiE, thiF, thiG,* and *thiH*), proposed to be a single transcription unit, are involved in thiamine biosynthesis (32). The ThiO protein of *E. coli* shows a limited sequence identity (12.5%) with *B. subtilis* GO.

By structural overlay, the GO structure was compared with that of other flavoprotein oxidases (see Table III). Based on structural and sequence homologies, GO can be classified as a member of the large GR family (all the family members adopt the Rossmann fold) (33, 34) and further into the subgroup GR_2, which was reported to show sequence similarity mainly within 30 residues in the N-terminal region (34). Our superposition procedure identified large, structurally homologous parts of GO with DAAO and MSOX (Table III). Although comparison of GO with dimethylglycine oxidase shows that 284 of 364 residues lie within the distance cut off of 3.5 Å, the r.m.s. deviation of those residues is high (1.84 Å), reflecting notable structural differences between GO and dimethylglycine oxidase. The enzymes pkDAAO, RgDAAO, and MSOX can be superimposed with a smaller r.m.s deviation (1.53–1.58 Å) with 222–256 of the 364 residues of the GO structure; this reflects the structural similarity of GO with both DAAOs and MSOX.

Compared with GO, the other GR_2 family members had either few residues lying within a 3.5-Å cut off, a high r.m.s deviation, or a low sequence identity of the superpositioned residues (see Table III), thus reflecting the structural and functional difference of these enzymes with respect to GO.

FAD Binding—Each GO monomer contains one noncovalently bound FAD molecule (1, 2). The FAD-binding patterns

TABLE I
Summary of data collection, data reduction statistics, and phasing statistics

	GO-glycolate, PSI/SLS/PX	GO-native, DESY/BW7B	GO-$Au(CN)_2$, rotating anode	GO-$K_2Pt(CN)_4$, rotating anode
Space group	$C222_1$	$P6_122$	$P6_122$	$P6_122$
Wavelength (Å)	0.97934	0.8463	1.54179	1.54179
Cell dimensions (Å) (*a*, *b*, *c*)	a = 73.71 b = 218.76 c = 217.80	$a = b$ = 139.32 c = 215.74	$a = b$ = 140.20 c = 215.88	$a = b$ = 140.18 c = 215.06
Resolution (Å)	1.8	3.0	3.1	3.5
No. reflections	581,432	153,016	327,517	188,451
No. unique reflections	159,578	25,398	42,479	29,476
Redundancy	3.6	6.0	7.7	6.4
Completeness[a]	98.2% (96.5%)	99.3% (99.8%)	99.6% (100%)	99.4% (99.8%)
R_{sym}[a,b]	4.6% (28.9%)	7.3% (48.4%)	11.2% (43.4%)	19.1% (38.8%)
R_{merged}[a,c]	7.1% (34.7%)	7.4% (32.2%)	8.7% (23.4%)	12.9% (22.5%)
I/σ[a]	15.85 (3.67)	16.6 (4.79)	16.71 (5.10)	10.16 (4.83)
No. heavy atom sites found by SOLVE			5	3
Phasing power of acentric (centric) reflections			0.65 (0.61)	0.82 (0.69)
FOM[d]			0.36	
FOM of acentric (centric) reflections after density modification			0.62 (0.66)	

[a] Values for the outer resolution shell are given in parentheses. Paul Scherer Institute/Swiss Light Source/Protein Crystallography beamline (PSI/SLS/PX), Deutsches Elektronen Synchrotron/Beamline BW7B (DESY/BW7B).
[b] $R_{sym} = \Sigma\Sigma_i|I_i - \langle I\rangle|/\Sigma\langle I\rangle$, where $\langle I\rangle$ is the mean intensity of N reflections with intensities I_i and common indices *h,k,l*.
[c] See Ref. 47.
[d] FOM, figure of merit.

TABLE II
Refinement statistics

	GO-glycolate
Resolution (Å)	20–1.8
Total no. non-hydrogen atoms	12,720
No. water molecules	1046
No. ligand atoms (FAD and glycolate)	232
No. reflections in working set	151,580
No. reflections in test set	8006
R_{work}[a] (%)	17.7
R_{free}[b] (%)	21.4
r.m.s. distance from ideal geometry	
Bonds (Å)	0,011
Angles (°)	1,32
Ramachandran plot[c]	
Total no. residues	1456
Most favored regions	1321
Additionally allowed regions	129
Generously allowed regions	4
Disallowed regions	2

[a] *R* factor = $\Sigma_{hkl}||F_{obs}| - k|F_{calc}||/\Sigma_{hkl}|F_{obs}|$, where F_{obs} and F_{calc} are the observed and calculated structure factors.
[b] For R_{free}, the sum is extended over a subset of reflections excluded from all stages of refinement.
[c] See Ref. 48.

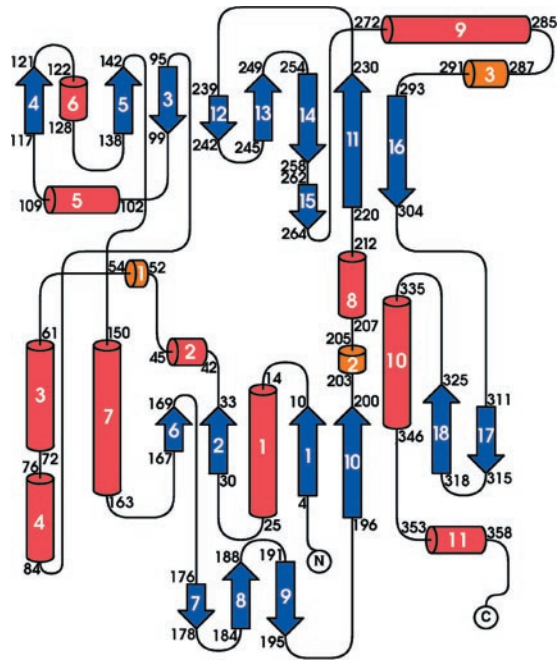

FIG. 2. **Secondary structure topology of GO.** α-Helices are shown in *red*; β-sheets are shown in *blue*, and the newly identified 3/10 helices are shown in *yellow*.

of GO, DAAO, and MSOX share an overall similarity; in all these enzymes the FAD-binding domain contains the conserved Rossmann fold βαβ motif (β1, α1, and β2) (33), which serves as a dinucleotide-binding motif (35). The central part of this consensus motif is the sequence G*X*G*XX*G (Gly^{11}, Gly^{13}, and Gly^{16} of helix α1) with the N-terminal end of helix α1 pointing toward the FAD pyrophosphate moiety, as observed for other dinucleotide-binding proteins (35). The binding of FAD in GO is that typical of the GR_2 subfamily (34); the prosthetic group adopts an extended conformation with the isoalloxazine ring located at the interface between the FAD-binding domain and the substrate-binding domain, facing with its *re*-side the inner part of the substrate-binding cavity. The cavity is located distant from the monomer-monomer interaction sites facing toward the bulk solvent. The whole cofactor is buried inside the protein (Fig. 1), and the isoalloxazine ring is not directly solvent-accessible. A similar situation was also observed in DAAO (10, 11), whereas in *p*-hydroxybenzoate hydroxylase the flavin benzene ring is exposed to the bulk solvent, allowing the flavin to adopt two different conformations (36). The large majority of the potential FAD hydrogen bonds are formed with the protein residues, thus resulting in a tight net as shown in Fig. 3, a K_d value for the apoprotein-FAD complex of $5 \pm 2 \times 10^{-8}$ M has been calculated.[2] The isoalloxazine ring is held in place by a hydrogen bond between its N-3H–C-4=O and the backbone of Gly^{48} and Met^{49}, whereas N-5 is within hydrogen bond distance to one of the oxygens of the inhibitor glycolate (this flavin position interacts with the backbone NH group of Gly^{52} and Ala^{49} in RgDAAO and pkDAAO, respectively, and with a water molecule in MSOX). The flavin N-1 is within hydrogen bond distance to the Arg^{329} backbone carbonyl oxygen in GO (such an

[2] L. Pollegioni, personal communication.

TABLE III
Superposition of GR_2 family members with glycine oxidase

Protein	PDB accession code (chain name)	No. residues within 3.5-Å cut off	r.m.s. deviation of residues within 3.5-Å cut off	Sequence identity of residues within 3.5-Å cut off
			Å	%
Dimethylglycine oxidase	1pj5	284	1.83	21.8
MSOX	1el5(a)	256	1.53	23.0
pkDAAO	1aa8(a)	249	1.54	18.4
RgDAAO	1c0p	222	1.58	20.7
p-Hydroxybenzoate hydroxylase	1bf3	154	1.46	12.3
Phenol hydroxylase	1foh(a)	150	1.70	12.0
Fumarate reductase	1d4d	148	1.75	20.3
D-Aspartate oxidase	1knr	144	1.64	16.7
Glucose oxidase	1cf3	134	1.72	19.4
Cholesterol oxidase	1mxt	128	1.54	17.1
Polyamine oxidase	1b37(a)	114	1.52	17.5
L-Amino acid oxidase	1f8r(a)	108	1.41	19.4

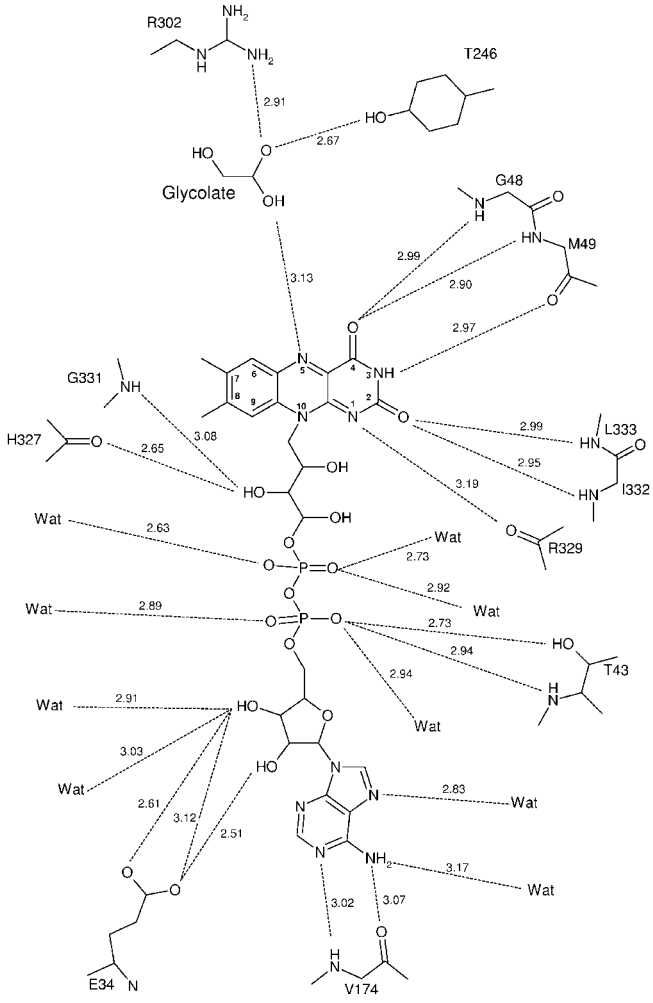

FIG. 3. **Schematic representation of the flavin-apoprotein interactions in GO.** View on the *si*-face of the flavin. Residues interacting with the cofactor via hydrogen bond are depicted. The hydrogen bonds are marked as *dotted lines* (distances in Å).

interaction is absent in pkDAAO and corresponds to RgDAAO Ser^{335} and MSOX Lys^{348}). The environment of the O-2 position is slightly different between GO and DAAOs. In GO the O-2 forms two H-bonds with the backbone NH group of Ile^{332} and Leu^{333} (Fig. 3). In pkDAAO O-2 interacts with a threonine and with the partial positive charge of a dipole from helix αF5 (10), and in MSOX the flavin O-2 forms a hydrogen bond to the side chain nitrogen of Lys^{348} (12).

These interactions serve to stabilize the electrophilic character of the flavin ring, and the negative charge of the anionic form of the semiquinone (1) and, probably, of the fully reduced flavin of GO. The benzene ring of the isoalloxazine moiety makes van der Waals contacts with a pocket formed by the antiparallel β-strands 11 and 15; the contacting residues are Ala^{45}, Ala^{46}, Ala^{47}, Gly^{224}, Cys^{226}, Tyr^{246}, Ala^{259}, Gly^{300}, and Arg^{302}. In particular, Arg^{302} is ~4 Å from the C-7 and C-8 position of the flavin. Most interesting, GO Gly^{300} occupies the same position as Cys^{315} in MSOX, the site of covalent flavinylation. The covalent attachment of the flavin cofactor to the apoprotein moiety requires the contribution of a base to act as a proton acceptor from the 8α-CH_3 group of FAD during tautomerization and possibly to generate the reaction thiolate from Cys^{315} (12). The proposed candidate is His^{45} in MSOX (in GO an alanine is instead present). Analogously to DAAO and MSOX, there are no acidic residues in the region surrounding the isoalloxazine ring.

The FAD diphosphate group forms one H-bond with Thr^{43} in GO. Five H_2O molecules are found at optimal hydrogen bonding distance with four of the phosphate oxygen atoms (Fig. 3). The side chain of the highly conserved GO Asp^{34} of the FAD-binding domain interacts via three strong hydrogen bonds with the two OH groups of the AMP ribosyl moiety. The adenine moiety forms hydrogen bonds to the backbone of Val^{174} and a water molecule (Fig. 3). Although different amino acids interact with AMP in GO, MSOX, and DAAO, the overall picture is similar.

Mode of Oligomerization—Native GO from *B. subtilis* is a stable 169-kDa homotetramer whose oligomerization state is not dependent on protein concentration in the 0.01–13 mg/ml concentration range (2). The molecular mass of GO in solution estimated from dynamic light scattering and blue native PAGE (37) is ~160 kDa and corresponds to the theoretical value of 173 kDa for the recombinant GO tetramer. Crystals of GO have the space group P6122 (hexagonal) and $C222_1$ (orthorhombic). In both space groups GO crystallized as a tetramer. The tetramers of both space groups are identical and have a 222 point symmetry. The tetramer of the hexagonal crystal is also identical to the one described previously (8). In the orthorhombic crystal, there are four molecules (monomers) in the asymmetric unit, which build two identical tetramers; the first tetramer consists of the monomers A and B and their symmetry mates A′ and B′ after applying the symmetry operator (x, $-y + 2$, $-z + 2$) on chain A and B; the second tetramer consists of chains C and D and their symmetry mates C′ and D′ after applying the symmetry operator ($-x$, y, $-z + 3/2$). The difference between the two tetramers is the orientation of the crystallographic axis with respect to the tetramer (see Fig. 4).

In detail, different surface regions are involved in contacts made by each monomer with the other three monomers in the

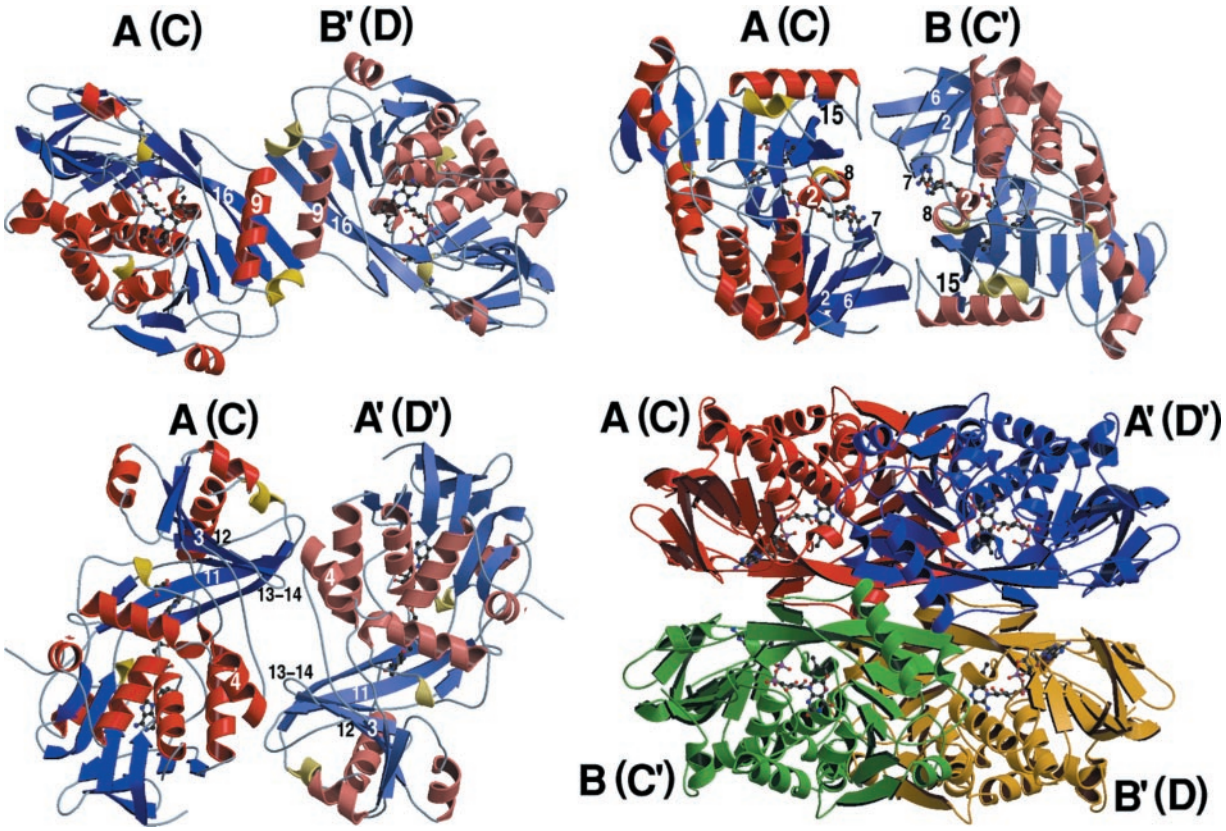

FIG. 4. **Different modes of monomer-monomer interaction of the four subunits of tetrameric GO.** Relevant regions are numbered. *A*, chain A of the four molecules of the ASU. *A′*, crystallographic symmetry-related molecule of *A*. *B*, chain B of the four molecules of the ASU. *B′*, crystallographic symmetry-related molecule of B. Not shown: the monomers *C* and *D* of the ASU make an additional tetramer with their crystallographic symmetry-related counterparts (*C′* and *D′*). For details see description in the text. *Right lower corner*, the two crystallographic tetramers are shown together with the chain identifiers. The crystallographic axis of the tetramer *ABA′B′* lies vertically and that of tetramer *CDC′D′* lies horizontally within the paper plane.

same tetramer. The interface between monomers A and B′ (and C and D) is largely because of residues from α9 and β16 of each subunit and buries a total surface of about 1770 Å^2. There are eight hydrogen bonds between the two monomers, formed by the following residues: Pro^{270}–Val^{204}, Leu^{272}–Met^{292}, Gly^{273}–Gln^{290}, and Lys^{283}–Glu^{276}. Apart from the last pair of residues, the hydrogen bonds are between main chain N and C atoms. Moreover, the Leu^{275} from α9 forms a hydrophobic pocket with the β16 residues Val^{294} and Phe^{297}. Most interesting, the side chain of Phe^{297} adopts two conformations. Interaction between monomers A and A′ (and C and D′) is due to residues belonging to loop β11–12, loop α4-β3, and loop β13–14 and buries a total surface area of about 1870 Å^2; no hydrogen bonds are present, but the loops fit together very tightly. The size of this contact area is about 250 Å^2 larger than that reported previously (8). The third interaction between monomers A and B (and C and C′) is due to residues from loops β15-α9, β2-α2, β6-β7, and Met^{208} from α8, with a total buried surface area of only about 975 Å^2. The accessibility from outside to the funnel leading to the active site of each monomer is not restricted by the quaternary structure of GO; the openings face the bulk solvent and are far away from each other. Moreover, the GO quaternary structure shows that interaction between the flavin cofactor of different subunits is not possible. Superposition of the four chains with LSQMAN shows that the r.m.s. deviation between the monomers (A–D) is in the 0.22–0.44 Å range. The r.m.s. deviation between the two tetramers (ABA′B′ and CDC′D′) is 0.35 Å. This result demonstrates that the two crystallographic tetramers are identical and that the r.m.s. deviation between tetramers is from the observed difference between the intrinsic structure of the monomers.

In order to modify the stable tetrameric structure of GO, different approaches have been used. The tetrameric state of GO is not affected by pH in the pH range 6.5–9.5, as determined by means of gel-permeation chromatography. Treatment with increasing concentrations of thiocyanate (up to 1 M) results in a decrease of the peak corresponding to the tetrameric GO, but a corresponding increase in a peak at ~46 kDa corresponding to the monomer was not observed. This result indicates that the lipophilic ion affects the stability of GO in solution but does not alter its monomer-monomer interaction. Tetrameric GO is also strongly resistant to proteolysis; treatment of GO (1 mg of protein/ml) with 10% (w/w) trypsin, chymotrypsin, or SV8 protease (at 25 °C and pH 8.5) for up to 4 h does not change its elution volume in gel-permeation chromatography. In contrast to GO, the dimeric oligomerization state of RgDAAO is affected by proteolysis (38). Only the N terminus of GO is sensitive to proteases. Western blot analysis and protein sequencing demonstrated that trypsin and chymotrypsin treatment, respectively, converted the 382 amino acids of recombinant GO monomer into a protein form that was shorter by 8–10 and 12–14 residues (lacking the His tag at the N terminus).

In contrast to this, the apoprotein form of GO is monomeric and rapidly converts to tetrameric holoenzyme upon addition of FAD.[2] Considering that the FAD cofactor is involved in many protein core contacts (see above) and that the conversion to the apoprotein form abolishes the CD signal in the near-UV region due to the tertiary structure of the holoenzyme, it was deduced that the organization of the quaternary structure follows holoenzyme reconstitution.

The Active Site—The active site of GO is a cavity delimited

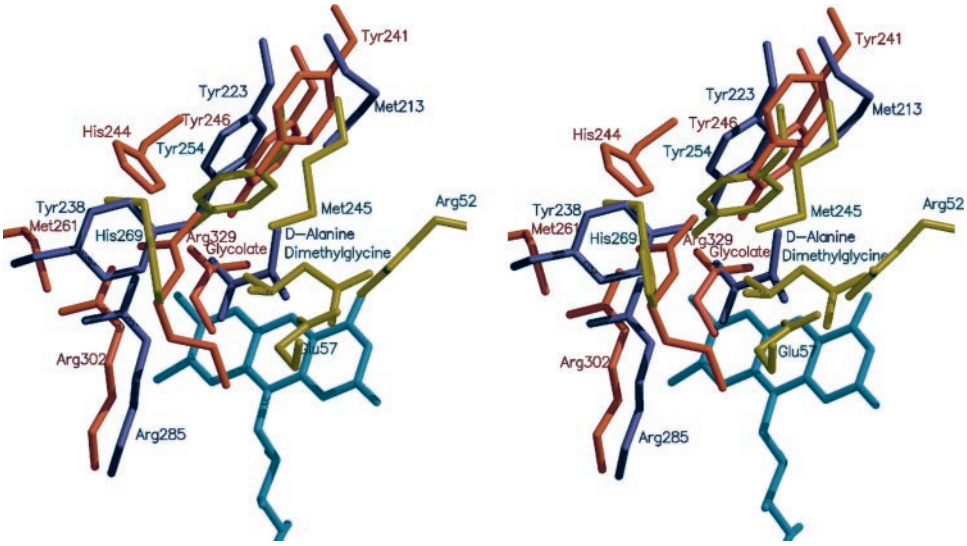

FIG. 5. **Stereo picture showing a comparison of ligand-active site interactions (*gray*, GO FAD).** *Blue*, RgDAAO in complex with D-alanine. *Red*, GO in complex with glycolate. *Yellow,* MSOX in complex with dimethylglycine. FAD cofactors of the three enzymes were superpositioned using LSQMAN.

by the two long β-strands, 11 and 16, bent around the isoalloxazine ring of the flavin and the two short β-strands, 13 and 14, located close to the substrate binding site; the flavin forms the bottom of the cavity (Fig. 5). The electron density is clearly seen for all atoms of the ligand glycolate in all four monomers of the asymmetric unit. The interactions can be described as follows: (*a*) Arg^{302} and Tyr^{246} form hydrogen bonds with one oxygen of the α-COO^- of the inhibitor glycolate (2.91 and 2.67 Å); (*b*) the second oxygen of the inhibitor α-COO^- group is at hydrogen bond distance to the N-5 of the FAD; (*c*) one terminal nitrogen of Arg^{329} and the main chain carbonyl of His^{244} form a hydrogen bond (3.02 Å) and are in close proximity to the α-COO^- of the bound ligand, probably preventing its rotation. Comparison of the structure of glycolate bound to GO with those of D-alanine in DAAO (11), dimethylglycine in MSOX (12), and acetylglycine in GO (8) shows that the α-COO^- of glycolate does not make two hydrogen bonds to the guanidyl group of GO Arg^{302} but instead that the ligand is unexpectedly rotated by ~120° and binds in a different orientation, which is observed in all four molecules of the ASU. This binding mode may be favored by the small size of glycolate, and probably could resemble the binding mode of glycine, which has approximately the same size as the inhibitor we used.

It is noteworthy that the substrate binding geometry of MSOX is reversed compared with DAAO and GO (Fig. 5). GO Tyr^{246}, which forms with its side chain oxygen a hydrogen bond to one of the α-COO^- oxygens of glycolate, is found at a position resembling that of RgDAAO Tyr^{223} (a residue involved, mainly by steric effects, in substrate binding) and of MSOX Tyr^{254} (whose role in substrate binding is considered marginal). GO Arg^{302} corresponds to RgDAAO Arg^{285} (and pkDAAO Arg^{283}) and to MSOX Arg^{52}; in all these enzymes, it is the residue that interacts with the α-COO^- of the substrate. In MSOX the movement of Arg^{52} following inhibitor binding induces a large replacement of a loop region that directs MSOX Glu^{57} into the active site (to bind MSOX Arg^{52}) (12). Concerning the modulation of the substrate specificity, GO Tyr^{241} is located at a position resembling that of MSOX Met^{245} and RgDAAO Met^{213} (Fig. 5). This latter residue was recently demonstrated to modulate the substrate specificity of yeast DAAO (39); the introduction of a positive charge at this position by site-directed mutagenesis provided a DAAO variant active on both neutral and acidic D-amino acids.

Most interesting, the loop found in pkDAAO and which was proposed by Mattevi *et al.* (10) to act as lid-controlling access to the active site, is absent in GO (as well as in RgDAAO and MSOX). The pkDAAO loop contains an important residue, Tyr^{224}, which is probably involved in substrate/product fixation (10). The RgDAAO Tyr^{238} side chain, which was also proposed to change its position in order to allow substrate/product exchange, is placed at a position similar to that in pkDAAO Tyr^{223}, GO Arg^{329}, and MSOX His^{269} (Fig. 5). The latter residue was primarily considered the active site base, although now a different role has been proposed (40).

No lid is evident in GO, but some side chain rearrangements occur upon inhibitor binding, in particular in Arg^{329} and Met^{261}. We proposed that His^{244} should be involved in a system to drive the protons outside the active site; a proton should be taken up from the substrate by the latter residue and transferred to Arg^{329} and to Met^{261} that is outside the active site. In GO, the following residues form the entrance to the active site: Ala^{259}, Thr^{260}, Met^{261}, Arg^{329}, His^{244}, Asp^{243}, and Cys^{245} (Fig. 6). Site-directed mutagenesis of Met^{261} (to Tyr and His) supports such a conclusion. The mutants have properties quite similar to the wild-type (similar V_{max}); the main change is a 10-fold increase in K_m for the substrates and in K_d for the inhibitors and a change of the flavin redox properties in the free enzyme form.[2] There is a striking difference between our structure and the conclusions derived by the unliganded structure (8) regarding the seal of the active site. Comparison of free GO with GO in complex with glyoxylate (Fig. 6) shows that the movements of residues Met^{261} and Arg^{329} do not fully protect the bound ligand from external solvent and thus the imine product from hydrolysis.

Effect of Different Carbon and Nitrogen Sources on B. subtilis Growth and on GO Expression—A previous report (8) showed that the *B. subtilis* mutant *thioO*$^-$ was unable to grow in a synthetic medium not containing thiazole. The growth curves of the wild-type strain of *B. subtilis* on minimal medium in the presence and in the absence of thiazole alcohol are identical (see Fig. 7), thus demonstrating that wild-type *B. subtilis* does not require the thiazole moiety of thiamine to grow. The activity level of GO during the time course of *B. subtilis* growth in the presence and in the absence of thiazole is constant and corresponds to the basal level (0.03 units/g cell).

We used a chemically defined growth medium to elucidate

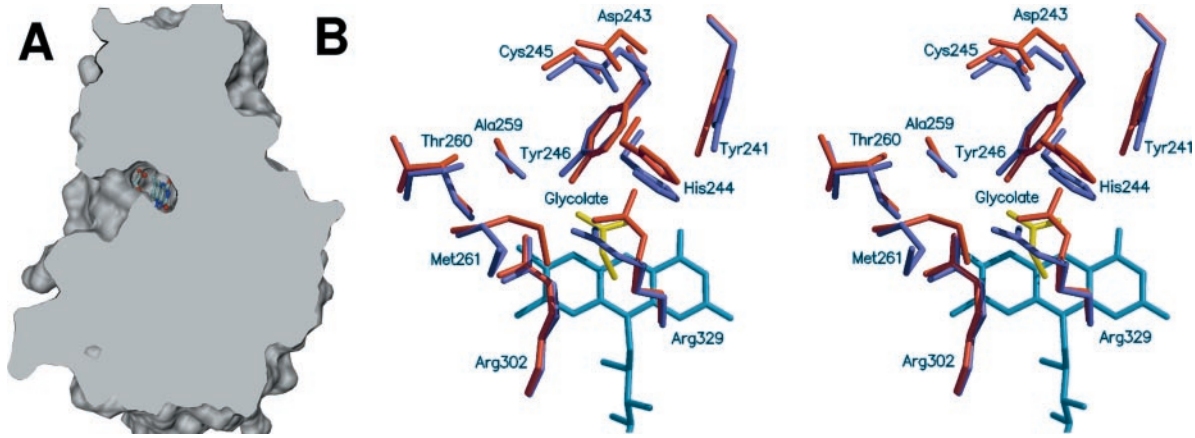

FIG. 6. *A,* side view of the substrate channel to the active site. Part of the flavin and the inhibitor glycolate are visible within the active site. *B,* comparison of the active site entrance between the free form (1ng4, *dark blue*) and the glycolate-complex form of GO (1ryi_a, *red*), showing a magnified view along the direction of the funnel leading to the active site. The glycolate is depicted in *yellow* and the GO FAD in *light blue*. Superposition was performed using SUPERIMPOSE (27).

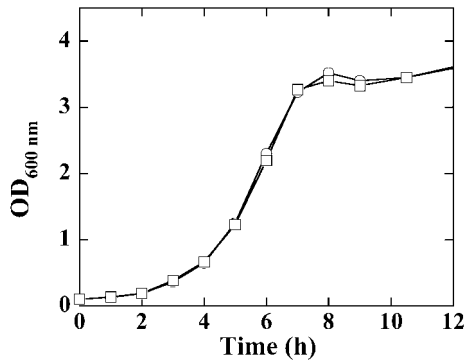

FIG. 7. **Effect of thiazole alcohol on the growth of wild-type strain of *B. subtilis*.** Growth of *B. subtilis* was performed in minimal medium in the absence (○) and in the presence (□) of 2 μM thiazole alcohol.

TABLE IV
Effect of carbon and nitrogen sources on the aerobic growth of B. subtilis on chemically defined media

The minimal medium contains 0.2% L-glutamine and M9 medium (in *parenthesis*), at 37 °C and 180 rpm.

	Carbon source (20 mM)			
Nitrogen source (18 mM)	Glucose	Glycine	Sarcosine	D-Alanine
NH_4Cl	+(+)	(−)	(−)	(+)
Glycine	+(−)	−		
Sarcosine	(−)			
D-Alanine	+(+)			
L-Glutamine			+	

the effect of nutrients on the level of GO synthesis. *B. subtilis* cells were grown on a minimal medium (that contains 0.2% L-glutamine), as well as on M9 medium (according to Ref. 8), supplemented with different carbon and nitrogen sources (see Table IV). Using M9 minimal medium, *B. subtilis* grows following the addition of ammonium chloride or D-alanine as a nitrogen source, whereas no growth is observed when either glycine or sarcosine are the sole nitrogen source. However, growth of *B. subtilis* was observed in the presence of both glucose and glycine using the minimal medium from Ref. 8 because of the presence of 0.2% L-glutamine in this chemically defined medium. Glycine cannot be used by *B. subtilis* as the sole carbon source in either M9 or minimal medium, although sarcosine supports *B. subtilis* growth as the carbon source only using the minimal medium (because it contains L-glutamine as the main nitrogen source, see above). On the other hand, the D-isomer of alanine can be efficiently used as a carbon source (even using the M9 medium) in the presence of ammonium chloride as a nitrogen source, and also as a nitrogen source with glucose as a carbon source. It is important to note that, with the only exception of GO, no enzymatic activities have been reported in *B. subtilis* that can efficiently and directly catabolyze D-alanine.

The level of GO activity and total GO protein expressed in *B. subtilis* was investigated for all the conditions reported previously that supported the growth of *B. subtilis* cells. In all cases, the GO activity in the crude extract is at the limit of detection; during all growth phases the amount of GO corresponds to the basal level of enzymatic activity (0.03–0.04 units/liter of fermentation broth). Most interesting, Western blot analysis showed that GO in the crude extract was always below the detection limit under these growth conditions (*i.e.* the GO expression is <0.03% of the total proteins present in the crude extract). The same result was also obtained when Western blot analysis was performed using the whole cells.

Effect of Phosphate and Thiamine Pyrophosphate on GO Activity—A previously detailed kinetic characterization of GO showed that the enzyme follows a classic Michaelis-Menten dependence of the reaction rate as a function of substrate concentration, without any indication of sigmoidal behavior (5). In the structure of GO reported previously (8), a phosphate ion was modeled into a buried, positively charged pocket formed by interaction of two monomers in proximity of the residues Arg^{89}, Arg^{254}, and Arg^{296}. In the orthorhombic crystal, all three corresponding sites, which lie between the monomer pairs AA′, BB′, and CD, were investigated; neither the sites that are located on a crystallographic axis (AA′ and BB′) nor those on a noncrystallographic axis (CD) show any indication of bound phosphate ions at these sites. In agreement with our crystallographic data, the addition of phosphate (in the 1–130 mM concentration range) does not affect the activity of GO.

Because of the proposed role in *B. subtilis* of GO in the biosynthesis of the thiazole moiety of thiamine (8) and of its tetrameric oligomerization state, the effect of the proposed final product (thiamine and thiamine pyrophosphate) of this synthetic pathway on the enzymatic activity of GO was also assessed. As reported previously for phosphate, even the addition of 0.1, 1, and 50 mM thiamine and thiamine pyrophosphate does not affect the activity of GO.

DISCUSSION

Amine oxidation is widespread in biology, and several different enzymes have evolved that catalyze these reactions. In the

present investigation we used a combination of structural and functional studies to clarify the physiological role of GO in *B. subtilis*. On the basis of the data presented here, we propose that the structure of *B. subtilis* GO resembles that observed for MSOX and DAAO and that both enzymes have a catabolic role, although in the specific mode of FAD and substrate binding different amino acids are involved. On the other hand, a different role of GO in the formation of the thiazole moiety of thiamine was recently proposed (8); this role requires that the imine product of dehydrogenation of glycine is trapped at the active site of GO with the thiocarboxylate produced by the following enzyme of the metabolic pathway, ThiS. This proposal is also supported by the sequence homology between GO and ThiO, a protein that has been suggested to catalyze this reaction in *R. etli* (31). This nucleophilic addition may occur before hydrolysis of the imine, which, when it is released from the enzyme, takes place immediately. If such a condensation reaction really occurs at the active site of GO (8), it should be more easily supported by a ping-pong kinetic mechanism of the GO reaction because the rate of product release from the reduced flavin form is known to be slower than that from the re-oxidized enzyme (5). Instead, we recently demonstrated that GO follows a sequential, ternary complex kinetic mechanism with glycine as well as with sarcosine and D-proline as substrate (5); the kinetic mechanism is consistent with the flavin reoxidation starting from the reduced enzyme-imino acid complex. Furthermore, comparison of the active site entrance of GO in complex with glycolate and in the free form (Fig. 6) does not show any seal of the active site that would prevent the hydrolysis of the imine product before release. The entrance of the substrate to the active site of GO is found to be on the solvent-accessible side of each monomer, far away from monomer-monomer contact areas. GO does not have a lid that controls substrate access and product release, a main difference in comparison to that observed in other known amino acid oxidases. The structural data do not clarify how GO can interact with ThiS and how the imine product can react with the thiocarboxylate intermediate bound to ThiS. Only further investigations concerning the structure of the proposed complex between GO and ThiS can provide a rationale for the proposed role of GO in thiamine synthesis if such a complex demonstrated a direct connection between the two active sites, together with a sealing from solvent of the GO active site.

A further obscure point that hardly correlates with the proposed role in the anabolic production of thiamine is represented by the (wide) substrate specificity of GO. Is it only an evolutionary memory? GO is active on many of the compounds specifically oxidized by DAAO, MSOX, and monoamine oxidase (1, 2). In addition, the V_{max} is similar to that of many of the substrates tested, because it is essentially due to the rate of product release from the reoxidized enzyme (5). The rate of flavin reduction by the substrate is similar among glycine and sarcosine (the best substrates of GO), and indeed the K_m value for sarcosine is slightly lower than for glycine (5).

An additional intriguing point pertains to the oligomeric state of GO. Why is GO tetrameric, whereas all the other members of the amine flavooxidase family are monomeric or dimeric (no other members of the GR_2 subfamily are tetrameric)? We demonstrated that GO does not show any allosteric behavior; the enzyme possesses classic Michaelis-Menten kinetics as a function of substrate concentration (5), and no effect on the enzymatic activity by phosphate, thiamine, and thiamine pyrophosphate is observed.

In order to clarify the role of GO in *B. subtilis*, the effect of different nitrogen and carbon sources on the growth and the induction of GO activity were also investigated. A wild-type strain of *B. subtilis* does not require thiazole to grow, thus confirming that it is able to synthesize thiamine. We also demonstrated that glycine and sarcosine, two putative *in vivo* GO substrates, do not support *B. subtilis* growth when used as the sole carbon or nitrogen source, whereas D-alanine can be used as the main carbon source (Table IV). This latter compound can be used only if it is catabolized by GO, because no other enzymatic activities have been reported in *B. subtilis* to deaminate D-amino acids. Otherwise, D-alanine could be converted to the corresponding L-isomer by an amino acid racemase (various racemases have been identified in *B. subtilis* genome, in particular a D-alanine racemase) and thus L-alanine should be used as a carbon source. This latter possibility is in good agreement with our experimental evidence showing that the amount of GO (activity and protein) is not increased in the absence of thiazole and using D-alanine as the sole carbon source, *i.e.* GO is not inducible. The evolution of the regulation of amino acid degradative enzymes in *B. subtilis* resulted in enzymes present at high levels in sporulating cells and spores, rather than preferentially expressed during nitrogen-limited growth (for a review see Ref. 41). Catabolite-repressed genes in *B. subtilis* are controlled by more than one global regulatory mechanism. Although none of the *Bacillus* catabolite repression mechanisms is understood at the molecular level, it is clear that they are not analogous to the cAMP-catabolite-responsive element-dependent mechanism that is operative in *E. coli* (for a review on catabolite repression and inducer control in Gram-positive bacteria, see Refs. 42 and 43). We performed a search for a 14-bp palindromic sequence element corresponding to the catabolite-responsive element (consensus sequence, TG(T/A)NANCGNTN(A/T)CA), which mediates catabolite repression in a number of *B. subtilis* genes (44). Catabolite-responsive elements show a striking variability in their sequence and position with respect to the transcriptional start sites of regulated genes. Two sequences similar to the consensus sequence for catabolite-responsive elements are found within the reading frame of the GO-coding gene (close to the 5′ start site); with respect to the observed deviations of such elements from the canonical sequence (at least at three positions), GO cannot be considered as a protein active in carbon catabolite pathways.

We also showed that glycine and sarcosine cannot be used as a nitrogen source, whereas D-alanine supports *B. subtilis* growth even in the absence of L-glutamine (Table IV). Despite the different ecological habitats and life cycles of *B. subtilis* and enteric bacteria, such as *E. coli*, only minor differences in the physiology of ammonium assimilation have been reported between these bacteria (45). *B. subtilis* has no assimilatory glutamate dehydrogenase activity; therefore, ammonium assimilation occurs solely by the glutamate synthase pathway (its synthesis is raised during nitrogen-limited growth). Glutamine is the best nitrogen source for *B. subtilis*, followed by arginine, and even ammonium is a good nitrogen source. Expression of the arginine, proline, and histidine degradative enzymes has been reported to be substrate-inducible in both *B. subtilis* and enteric bacteria (46). However, and in contrast to the case for *E. coli*, their expression is not subjected to nitrogen regulation in *B. subtilis*, raising the possibility that this bacterium does not contain any global nitrogen-regulatory system. Our results show that the expression of GO is not modified by the different nitrogen sources used and in particular not by glycine, sarcosine, and D-alanine even if this latter compound can be used as the main nitrogen source and allows *B. subtilis* growth. Taken together, our microbiology experiments exclude regulation of GO synthesis according to the composition of the medium in *B. subtilis* and therefore do not support a main role of GO in the

catabolic utilization of primary and secondary amines.

In conclusion, the structural and functional properties determined on GO demonstrate that it belongs to the amino acid oxidase class of flavoproteins (in particular to the GR_2 subfamily) and that it is characterized by a broad substrate specificity, low kinetic efficiency, and a unique and stable tetrameric oligomerization state (depending on FAD binding). The combination of these investigations does not clarify how GO is involved in thiamine biosynthesis (mechanistic limitations of this role have been also reported in Ref. 8), nor do the microbiology experiments support a main catabolic role for this flavooxidase in *B. subtilis*.

Acknowledgment—We thank Dr. Viviana Job for the enthusiastic work in the preliminary investigations on GO.

REFERENCES

1. Job, V., Marcone, G. L., Pilone, M. S., and Pollegioni, L. (2002) *J. Biol. Chem.* **277,** 6985–6993
2. Job, V., Molla, G., Pilone, M. S., and Pollegioni, L. (2002) *Eur. J. Biochem.* **269,** 1456–1463
3. Pilone, M. S. (2000) *Cell. Mol. Life Sci.* **57,** 1732–1747
4. Wagner, M. A., and Schuman Jorns, M. (1997) *Arch. Biochem. Biophys.* **342,** 176–181
5. Molla, G., Motteran, L., Job, V., Pilone, M. S., and Pollegioni, L. (2003) *Eur. J. Biochem.* **270,** 1474–1482
6. Porter, D. J. T., Voet, J. G., and Bright, H. J. (1977) *J. Biol. Chem.* **252,** 4464–4473
7. Wagner, M. A., and Schuman Jorns, M. (2000) *Biochemistry* **39,** 8825–8829
8. Settembre, E. C., Dorrestein, P. C., Park, J. H., Augustine, A. M., Begley, T. P., and Ealick, S. E. (2003) *Biochemistry* **42,** 2971–2981
9. Mattevi, A., Tedeschi, G., Bacchella, L., Coda, A., Negri, A., and Ronchi, S. (1999) *Structure* **7,** 745–756
10. Mattevi, A., Vanoni, M. A., Todone, F., Rizzi, M., Teplyakov, A., Coda, A., Bolognesi, M., and Curti, B. (1996) *Proc. Natl. Acad. Sci. U. S. A.* **93,** 7496–7501
11. Umhau, S., Pollegioni, L., Molla, G., Diederichs, K., Welte, W., Pilone, M. S., and Ghisla, S. (2000) *Proc. Natl. Acad. Sci. U. S. A.* **97,** 12463–12468
12. Trickey, P., Wagner, M. A., Jorns, M. S., and Mathews, F. S. (1999) *Structure* **7,** 331–345
13. Pawelek, P. D., Cheah, J., Coulombe, R., Macheroux, P., Ghisla, S., and Vrielink, A. (2000) *EMBO J.* **19,** 4204–4215
14. Sambrook, J., and Russel, D. W. (2001) *Molecular Cloning: A Laboratory Manual*, Cold Spring Harbor Laboratory Press, Cold Spring Harbor, NY
15. Kabsch, W. (1993) *J. Appl. Crystallogr.* **26,** 795–800
16. Terwilliger, T. C., and Berendzen, J. (1999) *Acta Crystallogr. Sect. D Biol. Crystallogr.* **55,** 849–861
17. Terwilliger, T. C. (2000) *Acta Crystallogr. Sect. D Biol. Crystallogr.* **56,** 965–972
18. Vagin, A., and Teplyakov, A. (1997) *J. Appl. Crystallogr.* **30,** 1022–1025
19. Collaborative Computational Project, Number 4 (1994) *Acta Crystallogr. Sect. D Biol. Crystallogr.* **50,** 760–763
20. Kleywegt, G. J., Zou, J., Kjeldgaard, M., and Jones, T. A. (2001) *International Tables for Crystallography, Vol. F*: *Crystallography of Biological Macromolecules* (Rossmann, M. G., and Arnold, E., eds) pp. 353–356, Kluwer Academic Publishers Group, Dordrecht, The Netherlands
21. Brünger, A. T., Adams, P. D., and Rice, L. M. (1997) *Structure* **15,** 325–336
22. Murshudov, G. N., Vagin, A. A., and Dodson, E. J. (1997) *Acta Crystallogr. Sect. D Biol. Crystallogr.* **53,** 240–255
23. Kabsch, W., and Sander, C. (1983) *Biopolymers* **22,** 2577–2637
24. Kraulis, P. J. (1991) *J. Appl. Crystallogr.* **24,** 946–950
25. Merritt, E. A., and Bacon, D. J. (1997) *Methods Enzymol.* **277,** 505–524
26. Philippsen A. (2003) *DINO: Visualizing Structural Biology*, Biozentrum, University of Basel, Basel, Switzerland (www.dino3d.org)
27. Diederichs, K. (1995) *Proteins Struct. Funct. Genet.* **23,** 187–195
28. Kleywegt, G. J., and Jones, T. A. (1997) *Methods Enzymol.* **277,** 525–545
29. Schreuder, H. A., Prick, P. A., Wierenga, R. K., Vriend, G., Wilson, K. S., Hol, W. G., and Drenth, J. (1989) *J. Mol. Biol.* **208,** 679–696
30. Karplus, P. A., and Schulz, G. E. (1987) *J. Mol. Biol.* **195,** 701–729
31. Miranda-Rios, J., Morera, C., Taboada, H., Davalos, A., Encarnacion, S., Mora, J., and Soberon, M. (1997) *J. Bacteriol.* **179,** 6887–6893
32. Van der Horn, P. B., Backstrom, A. D., Stewart, V., and Begley, T. P. (1993) *J. Bacteriol.* **175,** 982–992
33. Rossmann, M. G., Moras, D., and Olsen, K. W. (1974) *Nature* **250,** 194–199
34. Dym, O., and Eisenberg, D. (2001) *Protein Sci.* **10,** 1712–1728
35. Wierenga, R. K., Drenth, J., and Schulz, G. E. (1983) *J. Mol. Biol.* **167,** 725–739
36. Entsch B., and van Berkel, W. J. (1995) *FASEB J.* **9,** 476–483
37. Schägger, H., Cramer, W. A., and van Jagov, G. (1994) *Anal. Biochem.* **217,** 220–230
38. Pollegioni, L., Ceciliani, F., Curti, B., Ronchi, S., and Pilone, M. S. (1995) *Biochem. J.* **310,** 577–583
39. Sacchi, S., Lorenzi, S., Molla, G., Pilone, M. S., Rossetti, C., and Pollegioni, L. (2002) *J. Biol. Chem.* **277,** 27510–27516
40. Zhao, G., and Schuman Jorns, M. (2002) *Biochemistry* **41,** 9747–9750
41. Fisher, S. H. (1999) *Mol. Microbiol.* **32,** 223–232
42. Saier, M. H., Jr., and Ramseier, T. M. (1996) *J. Bacteriol.* **178,** 3411–3417
43. Saier, M. H., Jr., Chauvaux, S., Cook, G. M., Deutscher, J., Paulsen, I. T., Reizer, J., and Ye, J. (1996) *Microbiology* **142,** 217–230
44. Hueck, C. J., and Hillen, W. (1995) *Mol. Microbiol.* **15,** 395–401
45. Schreier, H. J. (1993) in *Bacillus subtilis and Other Gram-positive Bacteria: Biochemistry, Physiology, and Molecular Biology* (Sonenshein, A. L., Hoch, J. A., and Losick, R., eds) pp. 281–298, American Society for Microbiology, Washington, D. C.
46. Fisher, S. H. (1993) in *Bacillus subtilis and Other Gram-positive Bacteria: Biochemistry, Physiology, and Molecular Biology* (Sonenshein, A. L., Hoch, J. A., and Losick, R., eds) pp. 221–228, American Society for Microbiology, Washington, D. C.
47. Diederichs, K., and Karplus, P. A. (1997) *Nat. Struct. Biol.* **4,** 269–275
48. Laskowski, R. A., MacArthur, M. W., Moss, D. S., and Thornton, D. S. (1993) *J. Appl. Crystallogr.* **26,** 283–291